Identification of Vertical Profiles of Reflectivity from Volume Scan Radar Data

BERTRAND VIGNAL AND HERVÉ ANDRIEU

Division Eau, Laboratoire Central des Ponts et Chaussées, Nantes, France

J. DOMINIQUE CREUTIN

Laboratoire d'Etude des Transferts en Hydrologie et Environnement, Grenoble, France

(Manuscript received 15 December 1997, in final form 16 November 1998)

ABSTRACT

The vertical variability of reflectivity in the radar beam is an important source of error that interferes with a reliable estimation of the rainfall rate by radar. This source of error can be corrected if the vertical profile of reflectivity (VPR) has been previously determined. This paper presents a method for determining local VPRs from volume scan radar data, that is, from radar data recorded at multiple elevation angles. It is shown that the VPR directly provided by volume scan radar data differs from the true one, which can make it inappropriate to the correction of radar data for the VPR influence. The VPR identification method, based on the analysis of ratios of radar measurements at multiple elevations angles, is then described. The application conditions of the method are defined through sensitivity tests applied to a synthetic case. A ''real world'' case study allows performing a first evaluation of the proposed method. This analysis demonstrates that the identification of local VPRs and the correction for their influence at a scale of about 100 km^2 contributes to improving the reliability of rainfall measurement by radar. Moreover, it is shown that a correction of radar data based on identified VPRs performs better than a correction based on the VPRs directly deduced from volume scan radar data. This last point confirms the importance of the VPR identification stage in the correction of radar data for this source of error.

1. Introduction

The vertical structure of radar echoes in the radar beam is considered one of the dominant sources of error in the measurement of rainfall by radar (Joss and Waldvogel 1990). The effect of vertical variations of reflectivity is more pronounced for radars operating in difficult settings, such as mountainous regions (Joss and Lee 1995; Andrieu et al. 1997); these vertical variations contribute in any case to limiting the effective range of radar as a rainfall sensor (Koistinen 1991; Fabry et al. 1992). The requirement of accurate rainfall measurements led to an increasing interest for the correction of radar data from the influence of vertical profiles of reflectivities (hereafter VPR). Various approaches have been proposed to perform this correction. Climatological range-dependent corrections, depending on seasons (Koistinen 1991) or rain types (Collier 1986), were introduced first. Some methods are specifically devoted to brightband correction, where the bright band is the peak of reflectivity related to the melting layer (Klaassen 1988). Hardaker et al. (1995) used a melting layer model, while Fabry and Zawadzki (1995) deduced the statistical characteristics of bright bands from long-term observations of a vertically pointing radar. Numerous authors have suggested proceeding by two steps: i) determination of the VPR, and ii) correction of radar data using the determined VPR. Kitchen et al. (1994) proposed a VPR correction method relying on satellite images and ground meteorological data. In this method, an idealized representation of VPRs contains three components: the decrease of reflectivity in the upper part of the profile associated with a decrease of the precipitation water content with altitude, the brightband peak of reflectivity located just below the isotherm 0°, and the eventual increase of reflectivity due to orographic enhancement in the lower part of the atmosphere. The parameters defining these components are adjusted according to surface observations and infrared satellite data. Finally, Joss and Lee (1995) explored the difficult case of an Alpine mountainous setting where beam occultation combines with the VPR influence. The mean VPR was determined from volume scan data collected close to the radar, and the influence of beam occultation, expressed as a visibility coefficient, was deduced from the summation of a large number of radar images.

Corresponding author address: Dr. Hervé Andrieu, Div. Eau-Section Hydrologie en Milieu Urbain, Laboratoire Central des Ponts et Chaussees, BP19, F-44340 Bouguenais, France.
E-mail: Herve.Andr.eu@lcpc.fr

In a previous work, Andrieu and Creutin (1995) proposed an inverse method for retrieving VPRs from radar data recorded at two different elevation angles. Their main assumption was that the VPR is constant over the considered domain at a given time. A case study using ''real-world'' data (Andrieu and Creutin 1991; Andrieu et al. 1995) and a simulation study (Borga et al. 1997) led to the following conclusions about this algorithm: i) the VPR identification is accurate and contributes to improving radar estimation of the rainfall at the ground, and ii) the method may become inefficient when the assumption of VPR homogeneity is no longer satisfied. This paper describes the extension of the initial VPR identification method to volume scan radar data. This extension makes it possible to determine local VPRs at a spatial scale that is consistent with hydrological applications and resolves the limitations of the initial method due to the spatial heterogeneity of VPRs. From this perspective, this extension can contribute to improving the radar measurement of the rainfall rate. Moreover, the extended VPR identification method provides a means of deducing actual VPRs from volume scan radar sampling. Volume scan radar data do not directly provide the true VPR but rather a VPR estimate modified by the characteristics of the radar beam. The modifications consist of a smoothing and a vertical discretization depending on the resolution of the radar beam. This study considers the favorable case for which radar measurements can sample the whole volume of atmosphere. In particular, the influence of ground detections and beam blockages on the VPR identification procedure is not addressed.

As previously noted, the method presented in this paper complements an initial work presented in Andrieu and Creutin (1995) and Andrieu et al. (1995). Consequently, this paper focuses on the modifications introduced to account for volume scan radar data. Accordingly, it has been organized in the following way. Section 2 deals with the sampling of VPR through volume scan radar data and shows that volume scan radar data provide only apparent VPRs, that is, VPRs modified by radar beam characteristics. Section 3 addresses the extension of the VPR identification method to volume scan radar data. Section 4 presents the sensitivity tests performed to define its application conditions. Section 5 deals with a case study and covers data description, validation methodology, and validation results. Conclusions and recommendations are in section 6.

2. Volume scan radar sampling and VPR identification

This section recalls briefly the influence of VPR on the measurement of reflectivity and shows that volume scan radar data provide a degraded VPR, called the apparent VPR. The representativity of the apparent VPR is strongly related to the characteristics of the radar beam. Often the apparent VPR is not suited to correct radar data for the influence of VPR.

a. VPR influence on the measurement of rainfall by radar

The radar measurement of the reflectivity can be written in the following form:

$$\overline{Z}(x, A) = \int_{H^-(\theta_0, A)}^{H^+(\theta_0, A)} f^2(\theta_0, h) Z(x, h)\, dh, \qquad (1)$$

where notations have been simplified for the sake of convenience. The value $\overline{Z}$, the reflectivity measured by the radar, depends on the geographical location x, the elevation angle A, and the radar beamwidth θ_0; H^- and H^+ denote the lower and upper limits of the radar beam, respectively; f represents the partial integral of the power distribution of the radar beam at altitude h; and Z denotes the reflectivity that varies according to location x and altitude h. The rainfall rate is deduced from the reflectivity through the use of a Z–R relationship. It is assumed that Z can be broken down into two independent functions,

$$Z(x, h) = Z(x, 0) z_D(h), \qquad (2)$$

where $Z(x, 0)$ is the radar reflectivity at the ground level. The value $z_D(h)$ is called the vertical profile of reflectivity. The VPR is assumed constant and representative of the vertical variations of reflectivity in the geographic domain D. Combining Eqs. (1) and (2) leads to

$$\overline{Z}(x, A) = Z(x, 0) z_{Da}(h)$$

with

$$z_{Da}(h) = \int_{H^-(\theta_0, A)}^{H^+(\theta_0, A)} f^2(\theta_0, h) z_D(h)\, dh, \qquad (3)$$

where z_{Da}, hereafter called the apparent vertical profile of reflectivity, quantifies the difference between the reflectivity at ground and the reflectivity measured by the radar at the point (x, A). Here, z_{Da} depends on characteristics of the radar beam and the VPR itself. Andrieu and Creutin (1995) showed that the climatological approach is the only means of estimating z_{Da} using radar data at a single elevation angle. The availability of radar images at two or more elevation angles clears the way to identifying VPRs. The next paragraph discusses the link between VPRs and volume scan radar scans.

b. Volume scan radar scans and apparent VPRs

More and more often, normal operating conditions of weather radar include volume scanning. The procedure consists of recording about 5–20 PPIs at different elevation angles. This operating mode provides a 3D sampling of the atmosphere reflectivity. An apparent VPR can be easily extracted from volume scan data. However,

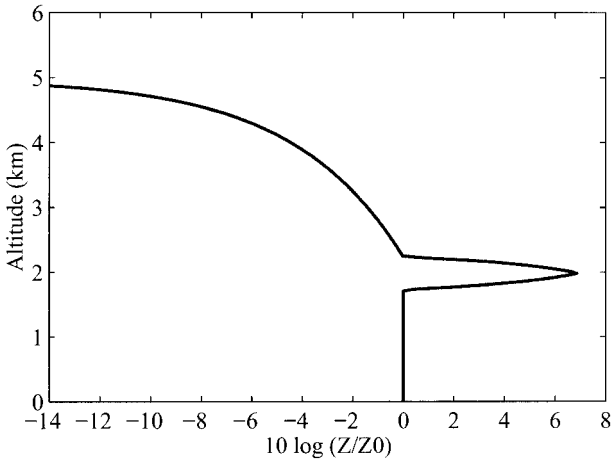

FIG. 1. Example VPR used in the framework of this paper in order to illustrate different aspects of the work. The brightband peak is at an altitude of 2 km above the radar.

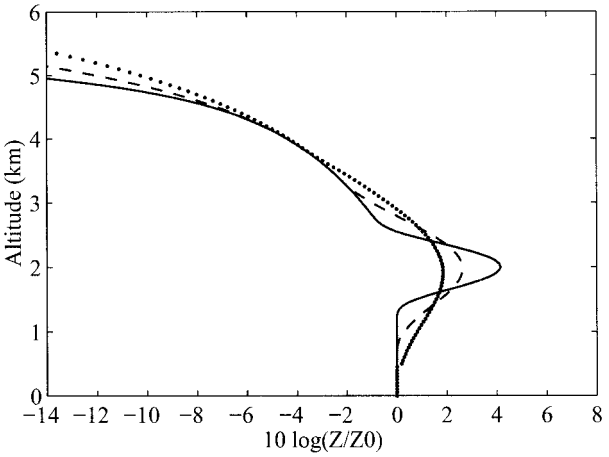

FIG. 2. Influence of the radar beam sampling on the VPR (θ_0 = 1.5°). Apparent VPRs associated with the example VPR at different distance ranges from the radar: 30 km (continuous line), 60 km (dashed line), and 90 km (dotted line).

this direct VPR estimate is subjected to several drawbacks.

1) Its quality of information deteriorates with range. At short distances from the radar, the smoothing effect of the radar beam remains negligible and the apparent VPR is not very different from the true VPR. The smoothing effect becomes more pronounced at increasing distances, and the apparent VPR turns out to be less representative of the actual VPR. The differences between the VPR and the apparent VPR can be illustrated by an example. Figure 1 shows a hypothetical, but realistic, VPR affected by a strong bright band located 2 km above the radar. Figure 2, which shows three apparent VPRs associated with this VPR at different ranges, 30 km, 60 km, 90 km, for a 3-dB radar beamwidth $\theta_0 = 1.5°$, confirms the importance of the radar beam smoothing. This beamwidth, larger than most of the recent radar beamwidths, is convenient for illustration purposes.
2) The limited number of antenna elevation angles introduces a discretization of the VPR, which lessens its accuracy. The influence of this discretization is shown in Fig. 3 that compares, at different distances from the radar, the continuous apparent VPR with the discretized apparent VPR sampled by a radar whose PPIs at successive elevation angles are separated by the 3-dB beamwidth ($\theta_0 = 1.5°$), the lowest elevation angle is 1°, and the elevation angle increment is 1.5°. Figure 3 displays that the number of informative vertical bins is reduced to 3 at 60 km and to 2 at 90 km, which makes the discretized apparent VPR very different from both the continuous apparent VPR and the true VPR shown in Fig. 1. The loss of information on the lowest part of the VPR due to the earth's curvature when the distance increases adds to the sampling effect.
3) At a given location, the vertical information provided

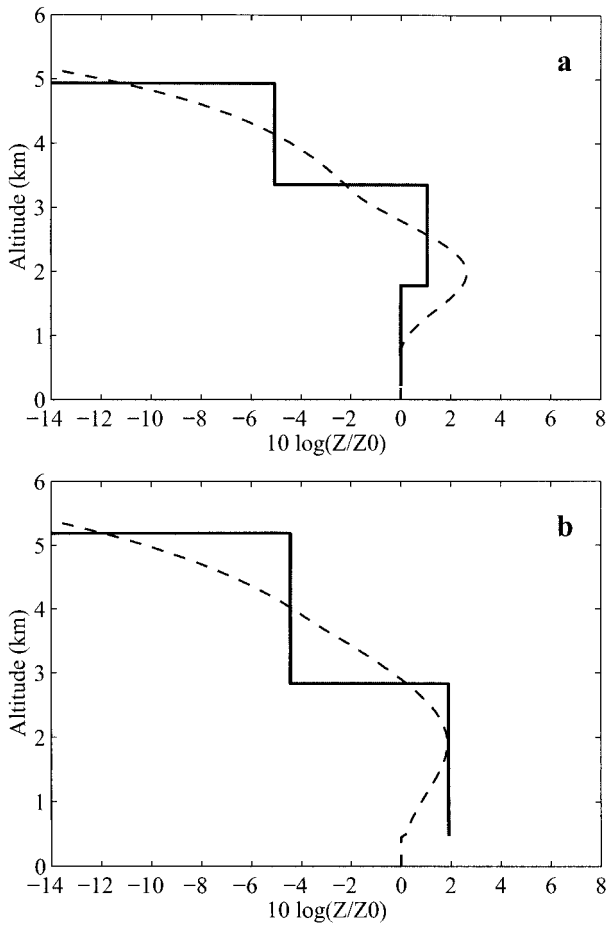

FIG. 3. Measurement of the example VPR by a radar performing volume scans according to the following conditions: $\theta_0 = 1.5°$, lowest elevation angle: $A_1 = 1.0°$, elevation angle increment: $\Delta A = 1.5°$. Comparison of the apparent VPR (dashed line) and the radar perception of the VPR (continuous line) at different distances from the radar: (a) 60 km; (b) 90 km.

by volume scan radar data does not allow the correction of the VPR's influence. As stated in Eq. (3), the lowest radar measurement depends both on the reflectivity value at the ground level and on the vertical variability of reflectivity in the radar beam. If the vertical radar bins do not overlap, there are no means to separate the influence of both effects, which prevents from correcting a radar measurement.

In conclusion, it has been shown that volume scan radar data do not provide the true VPR but the apparent VPR, that is, the VPR modified by the influence of the radar beam. Moreover, the previous remarks indicate that the efficiency of a method to determine VPR from volume scan radar data depends on its ability i) to filter horizontal variations of reflectivity and enhance the influence of vertical variations, and ii) to benefit from the property of radar data according to which the increase of the beamwidth and of the height of the beam axis with range provides indirect information on the vertical structure of the reflectivity.

3. Extension of the VPR identification method to volume scan data

This section deals with the VPR identification method, on which this work is based (Andrieu and Creutin 1995; Andrieu et al. 1995). The first paragraph recalls the principles of VPR identification from ratio curves of reflectivities or rainfall intensities. The second paragraph summarizes the inverse algorithm used to retrieve VPRs from ratio curves whereas the third paragraph introduces the discretized model. The last paragraphs address the data and parameters and the associated covariance matrices, respectively.

a. Principle of VPR identification

The basic assumption of the proposed method is that the VPR is invariant with the studied domain. The principle of the method consists of calculating the ratio of radar measurements at the same location and at different elevation angles versus distance. The introduction of ratios allows filtering the horizontal variability of radar reflectivity at the ground level and gives

$$q_z(x, A_1, A_i) = \frac{\overline{Z}(x, A_i)}{\overline{Z}(x, A_1)} = \frac{\displaystyle\int_{H^-(\theta_0, A_i)}^{H^+(\theta_0, A_i)} f^2(\theta_0, h) z_D(h)\, dh}{\displaystyle\int_{H^-(\theta_0, A_1)}^{H^+(\theta_0, A_1)} f^2(\theta_0, h) z_D(h)\, dh}, \tag{4}$$

where z_D is the VPR over the considered domain D, q_z is the ratio of reflectivities, and A_1 and A_i are the lowest and a higher elevation angles, respectively. This ratio can be a reflectivity or rainfall intensity ratio (related by $q_r = q_z^{1/b}$, with b being the exponent of the Z–R relationship).

The function q_z can be interpreted as the signature of the VPR modified by both the beam geometry and by the use of a ratio. A major limitation lies in the assumption of spatial invariance of the VPR. The availability of volume scan radar scanning makes this limitation less constraining by sampling the whole VPR within a shorter distance interval thanks to several ratio curves. However, the introduction of several ratio curves does not suppress the required assumption of spatial invariance of the VPR. At this point, it is not possible to define the area over which this assumption is correct. It mainly depends on the meteorological situation and should be more easily satisfied for stratiform rain events than for rain events displaying convective rain cells. A more detailed study of the spatial variability of VPRs based on the analysis of i) a series of radar data recorded at high elevation angle or ii) data provided by a vertically pointing radar would help to define this area for different types of rain events and different temporal integrations of radar data. Figure 4 displays the ratio curves of rainfall intensities associated with the reference VPR of Fig. 1 and the same radar features. The indications (A_k/A_1) associated with the different curves mean that they are obtained by dividing radar data at the elevation angle A_k by radar data at the elevation angle A_1. A ratio value over one indicates that the radar reflectivity at elevation number k is higher than the lowest reflectivity. In order to facilitate the interpretation of ratio curves, Fig. 4a shows the ratio curve obtained with two elevation angles (1.0° and 1.5°) in the distance interval from 0.0 to 100 km. Figure 4b shows the ratio curves between 30 and 50 km. At this short distance, the beam diameter is not very large and most of the radar measurements are below the echo-top altitude. Within this distance interval, radar data at elevations 1.5°, 2.5°, and 3.5° include the bright band, leading to ratio values exceeding 1. Figure 4b can be seen as the superposition of different segments of Fig. 4a. Figure 4c represents the ratios obtained in the distance interval (60 km, 90 km). The number of PPI images sampling the VPR is reduced to 4. Radar data at elevation 1.5° are the only ones able to sample the bright band. The qualitative comparison of Figs. 4c and 4b gives the impression that ratio curves of the former are less informative than ratio curves of the latter.

b. The VPR identification algorithm

Given the observed reflectivity or rainfall intensity ratios, the VPR identification consists of retrieving the VPR that best reconstitutes the experimental values of ratios according to the theoretical model defined by Eq. (4). The method chosen to solve this inverse problem belongs to inverse theory (Menke 1989) and the algorithm used in this work is the one proposed by Tarantola and Valette (1982a). The solution minimizes the following expression:

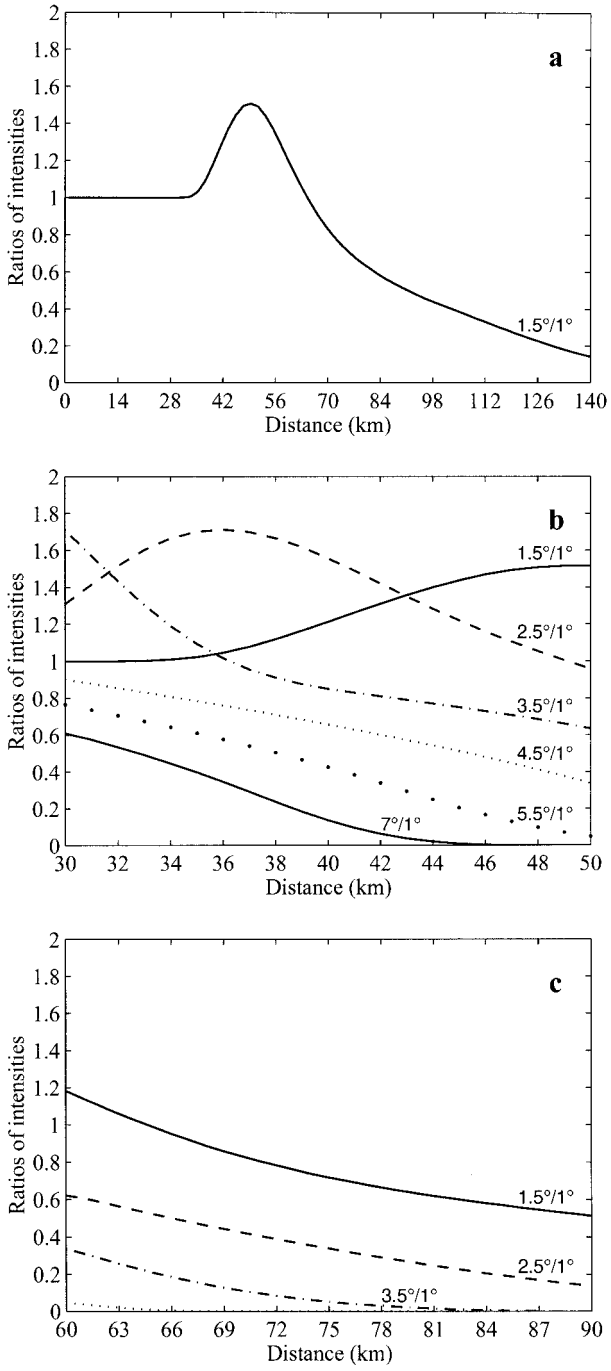

FIG. 4. Example of ratio curves of intensities associated with the example VPR: (a) the distance interval is (30 km, 50 km), whereas for (b) the distance interval is (50 km, 80 km). The numbers associated with each curve represent the higher elevation angle and the lower elevation, respectively.

$$\Phi(\mathbf{z},\mathbf{q}) = (\mathbf{z}-\mathbf{z}_0)^{\mathrm{T}}\mathbf{C}_z^{-1}(\mathbf{z}-\mathbf{z}_0) + (\mathbf{q}-\mathbf{q}_0)^{\mathrm{T}}\mathbf{C}_q^{-1}(\mathbf{q}-\mathbf{q}_0)$$
$$\mathbf{q} = m(\mathbf{z}), \qquad (5)$$

where Φ is the likelihood function and m is the theoretical model relating the vector of ratios $\mathbf{q}$ to the vector of the discretized VPR $\mathbf{z}$. Here, $\mathbf{q}_0$ denotes the vector of observed ratios, $\mathbf{z}_0$ is the a priori VPR, and $\mathbf{C}_q$ and $\mathbf{C}_z$ are the covariance matrices of ratios q and VPR components $\mathbf{z}$, respectively. The letter T signifies transpose. The statistical distributions of both $\mathbf{q}$ and $\mathbf{z}$ are assumed to be Gaussian. Menke (1989) demonstrates that the solution vector $\mathbf{z}'$ satisfies

$$\mathbf{z}' = \mathbf{z}_0 + \mathbf{C}_z\mathbf{M}^{\mathrm{T}}(\mathbf{M}^{\mathrm{T}}\mathbf{C}_z\mathbf{M} + \mathbf{C}_q)^{-1} \times [\mathbf{q}_0 - m(\mathbf{z}') + \mathbf{M}(\mathbf{z}' - \mathbf{z}_0)], \qquad (6)$$

where $\mathbf{M}$ is the matrix of partial derivatives of the model m. If the model m is nonlinear, Eq. (6) can be solved using an iterative method,

$$\mathbf{z}_{k+1} = \mathbf{z}_0 + \mathbf{C}_z\mathbf{M}_k^{\mathrm{T}}(\mathbf{M}_k^{\mathrm{T}}\mathbf{C}_z\mathbf{M}_k + \mathbf{C}_q)^{-1} \times [\mathbf{q}_0 - m(\mathbf{z}_k) + \mathbf{M}_k(\mathbf{z}_k - \mathbf{z}_0)], \qquad (7)$$

in which $\mathbf{z}_k$ constitutes the result of the kth iteration and $\mathbf{M}_k$ the matrix of partial derivatives at point $\mathbf{z}_k$. Further information about the stability, convergence, and uniqueness of the solution of such nonlinear problems can be found in chapter 9 of Menke (1989) and in Tarantola and Valette (1982a,b). The general case of inverse problems dealing with non-Gaussian statistics is addressed by Tarantola (1987). In the present study, it is assumed that data errors and residuals between a priori and true values of parameters are Gaussian. This hypothesis is checked in paragraph 5c.

Before applying this algorithm to the VPR identification, let us consider the a priori information and the nature of the studied problem. The a priori information is formed by the vector $\mathbf{z}_0$ and its associated covariance matrix $\mathbf{C}_z$. It contains the initial knowledge of the parameters to identify (i.e., the VPR) and the level of confidence that can be ascribed to this knowledge. The solution provided by the inverse algorithm results from a compromise between two extreme states: i) a solution that perfectly fits the observed data through the theoretical model and ii) a solution remaining very close to the a priori information on the parameters. The assistance provided by this a priori information actually depends on the nature of the problem. If the observed data are insufficient or if the confidence in the data (as defined by the covariance matrix $\mathbf{C}_q$ is weak, the problem is then underdetermined and the a priori information assumes a dominant role. If the problem is overdetermined (very good quality data in sufficient number), the solution no longer depends on the a priori information. The particular case of the VPR identification is illustrated in Fig. 4. Close to the radar (Fig. 4b) numerous values of the ratios are available, which means that the VPR variations are indirectly but well described by ratio curves, which could make the problem overdetermined. As shown in Fig. 4c, the increase of distance contributes to decrease the number of useful ratios. Moreover, the evolution of ratios versus distance is smoother. As illustrated by the comparison of Figs. 4b and 4c, the information available to deduce the VPR from ratios

deteriorates and the a priori VPR assumes greater importance. Depending on radar data characteristics, it may occur that the VPR identification is heterogeneously determined, which means that a part of the VPR is well sampled while the other part is not correctly seen. For example, due to the earth curvature and to the beam altitude increase, the lowest part of the VPR is less often sampled by the radar beam as the distance increases. In the same manner, if volume scans are composed of PPI at a reduced number of elevation angles (3 or 4), the VPR identification becomes heterogeneously determined, with the higher part of the VPR being less often sampled or sampled by less informative data (sampled by a larger diameter beam). In conclusion, the practical implementation of the VPR identification method is of importance, insofar as it exerts an influence on the solution.

c. The discretized model

The VPR is discretized and represented by the vector $\mathbf{z} = (z_1, \ldots, z_{n_z})$, where n_z is the number of elements at vertical intervals Δh. The vector of data regroups the values of all the observed ratios; it is written $\mathbf{q} = [(q_{2,1}, \ldots, q_{2,n_q}), \ldots, (q_{n_e,1}, \ldots, q_{n_e,n_q})]$, where n_e is the number of elevation angles and n_q is the number of points on each observed ratio curve. The ratios are expressed by the following formula:

$$q_{i,j} = \left[\frac{\sum_{k=1}^{k=n_z} \phi_k(x_j, A_i) z_k}{\sum_{k=1}^{k=n_z} \phi_k(x_j, A_1) z_k} \right]^{1/b}, \tag{8}$$

where the coefficient ϕ_k represents the contribution of the received power associated with the kth VPR component at the distance x_j for the elevation angle A_k [see Andrieu and Creutin (1995), appendix A, for the expression of these coefficients], $b = 1$ for a ratio of radar reflectivities, or b is the exponent of the Z–R relation for a ratio of intensities. In Eq. (8) the radar data at the lowest elevation angle (A_1) are always kept in the denominator to avoid the possibility of the ratio to take infinite values. Not all of the ratios are actually used, which could be determined using radar data at n_e different elevations. Vignal (1998) showed theoretically that the introduction of additional combinations of ratios does not provide any additional information as all the radar data have already been taken into account.

d. Ratios and covariance matrix of ratios

The VPR identification is applied to a zone of the radar image containing several pixels at the same distance from the radar. The ratio at a given distance is then estimated as the mean of all the individual ratios at this distance. The covariance matrix of ratios describes the statistical features of the errors of observed ratios. It is likely that nearby errors are correlated. The covariance matrix of ratios differs from that of the initial work by the introduction of the correlation between errors of ratios at the same distance, but associated with different ratio curves,

$$\begin{aligned} \sigma^q_{i,j} &= \alpha_q q_{i,j} + \beta_q \\ \operatorname{cov}(q_{i,j}, q_{k,l}) &= \sigma^q_{i,j} \sigma^q_{k,j} \exp\left[-\frac{(x_j - x_l)^2}{D_x^2} \right] \\ &\quad \times \exp\left[-\frac{(i-k)^2 \Delta h^2}{D_h^2} \right], \end{aligned} \tag{9}$$

where the standard deviation $\sigma^q_{i,j}$ of the measurement error of the ratio $q_{i,j}$ is a linear function of the same ratio introducing two parameters α_q and β_q. The parameter α_q is equivalent to the coefficient of variation of the statistical distribution of the ratio error, and β_q is used mainly to keep $\sigma^q_{i,j}$ positive when the ratio is equal to zero. The covariance expression is consistent with the hypothesis of normal distributions and D_x and D_h are the horizontal and vertical decorrelation distances of errors of ratios, respectively.

e. The a priori VPR and the associated covariance matrix

An effective choice consists of selecting the discretized apparent VPR as the a priori VPR $\mathbf{z}_0$. In practice, a discretized apparent VPR is available for each pixel of the considered sector, with the a priori VPR being obtained by calculating the mean value of all these discretized apparent VPRs. The VPR identification method is the technique of choice for refining the vertical variations captured by radar data by taking into account the additional information contained in the ratio curves.

The a priori covariance matrix $\mathbf{C}_z$ of the parameters is the covariance matrix on the errors between the a priori VPR and the true (and unknown) VPR. Indirectly, it constitutes a means of constraining more or less the VPR components about their a priori values. In order to correctly initialize the covariance matrix on the parameters, it is necessary to be able, even intuitively, to appreciate whether the problem to be solved is overdetermined or underdetermined. According to the brief analysis of section 3b, it appears interesting to relate the standard deviation of a VPR component to the quality of its sampling by radar data. This standard deviation is thus expressed by the following expression:

$$\begin{aligned} \sigma^z_i &= \alpha_z \frac{F(i)}{\max[F(i)]} z_i + \beta_z \\ F(i) &= \sum_{j=1,n_q;k=1,n_e} \phi_i(x_j, A_k), \end{aligned} \tag{10}$$

where $\phi_i(x_j, A_k)$ has been defined after Eq. (8) and α_z and β_z are two parameters. The function F determines the quality of the sampling of the VPR components by

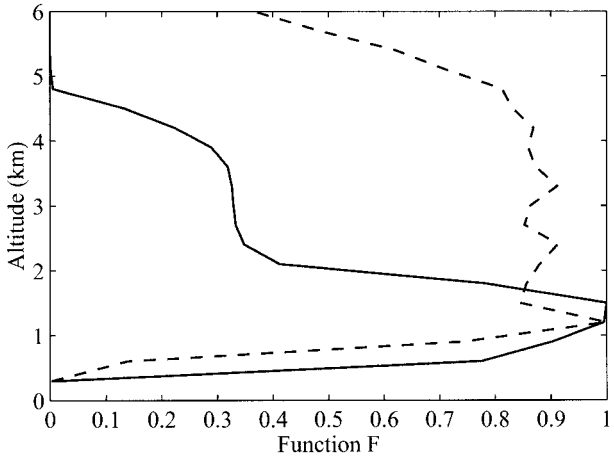

FIG. 5. Illustration of the function F used to initialize the standard deviation of the VPR components: the radar performs PPI at two elevation angles: 1° and 3° between 20 and 80 km (continuous line); the radar operates a volume scan scan (Table 1), with the ratio curves being accounted for between 40 and 60 km (dashed line).

quantifying how often a VPR component is illuminated by the radar beam. Introducing the term ϕ instead of simply counting the number of samples corresponds to the weighing of each sampling of a VPR component according to its location in the radar beam. Normalizing $F(i)$ by its maximum value over all of the VPR components allows attributing the coefficient of variation α_z to the best sampled VPR component. Figure 5 exemplifies the function F in two particular cases. The continuous line illustrates radar operation conditions leading to oversampling of the lower part of the VPR and to undersampling of the higher part of the VPR. The dashed line is related to a more homogenous sampling of the VPR components. The observed differences between the two cases depend on the radar operation conditions and on the distance interval. Figure 5 confirms the relevance of taking the quality of sampling in the a priori standard deviation of parameters into account. This expression can be used for the automatic determination of the standard deviation of the errors on the VPR component as a function of the radar operation conditions. An exponential model, consistent with the Gaussian hypothesis, has been selected for the covariance

$$\mathrm{cov}(z_i, z_j) = \sigma_i^z \sigma_j^z \exp\left[-\frac{(i-j)^2 \Delta h^2}{D_z^2}\right], \qquad (11)$$

where z_i and z_j are components of the VPR, and of respective standard deviations of error σ_i^z and σ_j^z, with D_z being the decorrelation distance.

4. Sensitivity analysis of the VPR identification method

The sensitivity tests are herein similar to those in the initial work (Andrieu et al. 1995) and can be summarized as follows. A synthetic VPR, called the reference VPR, is used to calculate ratio curves of rain intensities. These ratio curves serve to identify the VPR. The accuracy of the resulting VPR is quantified by comparing the identified VPR to the true VPR. The quality of the result is evaluated by calculating the deviation between the identified and the true VPR. Sensitivity tests have been performed using the two hypothetical VPRs that illustrate common situations: the example VPR shown in Fig. 1, characteristic of a bright band, and a VPR that introduces a regular decrease in the reflectivity with altitude. An example of identification of this example VPR is displayed in Fig. 6. Figure 6b shows that the ratio curves obtained with the identified VPR are closer to the ratio curves associated with the true VPR than

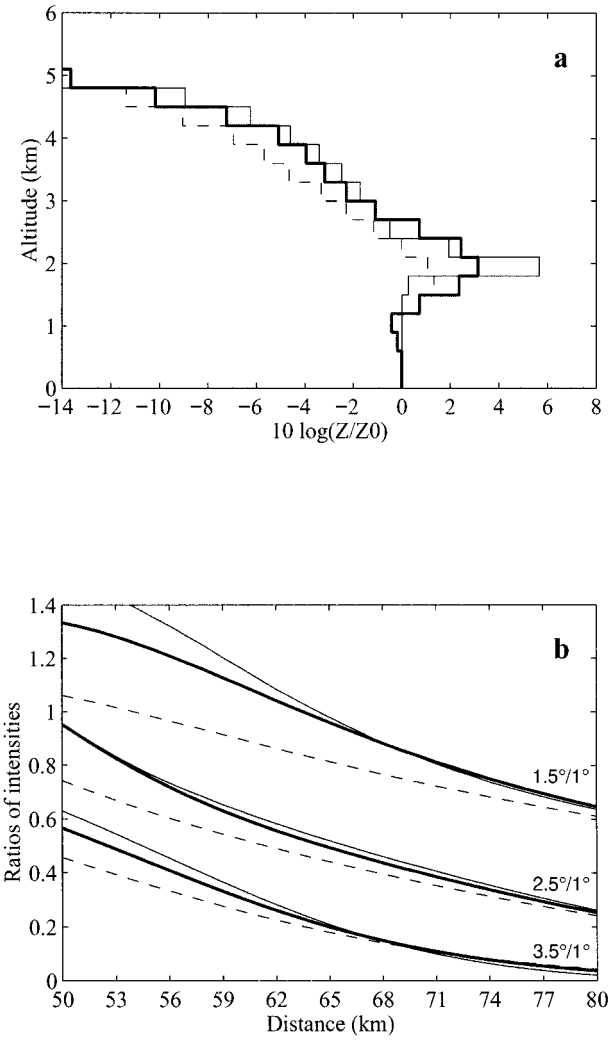

FIG. 6. Example of VPR identification: (a) representation of VPRs: a priori (dashed line), identified (thick continuous line), true (thin continuous line); (b) curves of ratio of intensities: observed (thin continuous line), corresponding, respectively, to the a priori VPR (dashed line), the identified VPR (thick continuous line), and the true VPR (thin continuous line).

the ratio curves obtained with the a priori VPR. As illustrated by Fig. 6a, the identified VPR appears as a better estimate of the true VPR than the a priori VPR. This paragraph summarizes the main conclusions of these sensitivity tests, with a detailed presentation being provided in Vignal (1998). The standard values of the parameters (Table 1) correspond to the setting of the case study described in section 5.

a. Ratios and associated covariance matrix

The sensitivity tests concern both the characteristics of ratios curves and the parameters of the covariance matrix. It first appears that both D_x and D_h exert a negligible influence on the obtained results, which can be explained by the very good continuity of ratios, both in distance and in altitude. These parameters are held equal to zero and the covariance matrix of the errors of the ratios becomes diagonal. According to previous findings, it is confirmed that an a priori overestimate of the standard deviation of the error of the ratios (σ^q) is better accepted by the algorithm than an underestimate. The availability of radar data at n_e different elevation angles makes it possible to calculate a large number of ratio curves [$n_e(n_e + 1)/2$]. The sensitivity analysis confirms that it is not necessary to take into account all of these combinations. The identification efficiency stabilizes with the ($n_e - 1$) ratio curves, obtained by dividing radar data at different elevation by the radar datum at the same point and at the lowest elevation angle. This finding confirms the theoretical result (Vignal 1998) showing that these ($n_e - 1$) ratio curves form a basis of ratios curves.

The efficiency of the identification method certainly depends on two major points. i) First, the type of rain event, frontal or convective, which induces the spatial variability of the VPR; ii) then, for a given rain event, the geographic zone where the VPR is to be determined. The influence of the former point is not addressed in the present work and could be the matter of a complementary study. The latter is a key point in the identification procedure insofar as it contributes to its over- or underdetermination. In terms of ratio curves, this zone is characterized by the interval [$d_{\min}$, $d_{\max}$], where $d_{\min}$ and $d_{\max}$ are the minimum and maximum distances from the radar, respectively. For the sake of convenience, the geographic zone can be equivalently defined by two variables: i) the mean distance from the radar, ($d_{\min} + d_{\max}$)/2, and ii) the distance interval, ($d_{\max} - d_{\min}$). The value to be ascribed to these two variables results from a compromise between two contradictory aspects: i) maintaining a distance interval as small as possible in order to satisfy the assumption of VPR homogeneity and ii) making the distance interval as large as possible in order to ensure that the ratios curves sample correctly the VPR. Actually, this compromise depends heavily on the mean distance from the radar, which simultaneously make the apparent discretized VPR (used as the a priori VPR) farther from the actual VPR and the ratio curves less informative as the distance increases. The influence of the two variables, mean distance and distance interval, on the efficiency of the VPR identification has been studied in the particular case of the reference VPR of Fig. 1 with the following radar characteristics: a 3-dB beamwidth $\theta_0 = 1.5°$, the lowest elevation angle $A_1 = 1°$, and the increment elevation angle $\Delta A = 1°$. The efficiency of the VPR identification can be evaluated by the criterion

$$E = 100\left[1 - \frac{\text{rmsd}(\mathbf{z}, \mathbf{z}^*)}{\text{rmsd}(\mathbf{z}, \mathbf{z}_0)}\right], \tag{12}$$

where rmsd($\mathbf{z}$, $\mathbf{z}_0$,) is the root-mean-square deviation between the a priori VPR $\mathbf{z}_0$ and the true VPR $\mathbf{z}$ and rmsd($\mathbf{z}$, $\mathbf{z}^*$) is the root-mean-square deviation between the identified VPR $\mathbf{z}^*$ and $\mathbf{z}$. This criterion E represents the reduction percentage of the initial rmsd provided by the VPR identification. If this criterion is lower than 10%, the identification is considered inefficient. The obtained results are displayed in Fig. 7, which illustrates

TABLE 1. Standard values of the parameters adopted for the sensitivity test of the VPR identification method. The different parameters associated with ratios are defined in section 3d after Eq. (9), whereas the parameters attached to the a priori VPR are defined in section 3e after Eq. (11).

Radar parameters:
Beamwidth at 3 dB: 1°
Elevation angles: 1°, 1.5°, 2.5°, 3.5°, 4.5°, 5.5°, 7.0°
Ratio curves:
$\sigma^q = 0.12q + 0.05$
$D_h = 0.0$ and $D_x = 0.0$
Distance interval: [50 km, 80 km]
A priori VPR:
$\Delta h = 0.3$ km
$\sigma^z = 0.7$, $D_z = 0.6$ km

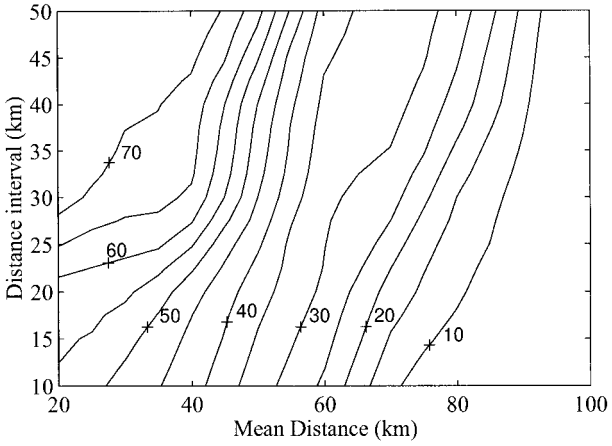

FIG. 7. Influence of the mean distance and the distance interval on the efficiency [defined in Eq. (12)] of the VPR identification procedure.

TABLE 2. Influence of radar features and brightband altitude on the useful distance of the VPR identification method.

Altitude of the bright-band peak	$\theta_0 = 1.5°$ $\Delta A = 1.5°$ $A_1 = 1.0°$	$\theta_0 = 1.5°$ $\Delta A = 0.75°$ $A_1 = 1.0°$	$\theta_0 = 1.0°$ $\Delta A = 1.0°$ $A_1 = 0.5°$	$\theta_0 = 1.0°$ $\Delta A = 0.5°$ $A_1 = 0.5°$
1.5 km	about 70 km	about 80 km	>100 km	>100 km
2.0 km	about 80 km	about 90 km	>120 km	>120 km
2.5 km	about 90 km	100–110 km	>120 km	>140 km

the efficiency of the VPR identification versus the mean distance and the distance interval. For instance, a VPR identification performed at a mean distance of about 60 km with a distance interval of 20 km is as efficient as an identification performed at 75 km, with the distance interval close to 50 km. More generally, the results of Fig. 7 have led to the following conclusions. This test clearly shows that the identification efficiency declines with range and that the modification of the identification conditions can only partially compensate for this range effect. In the context of the sensitivity tests, up to a distance of about 60 km from the radar, the criterion E takes a value larger than 30% if the distance interval does not exceed 30 km: the VPR identification method makes it possible to significantly improve the VPR seen by the radar. For longer distances, within the range 60–85 km, the criterion E stands between 10% and 30%. It means that the VPR identification algorithm becomes less efficient in improving the VPR seen by the radar and a distance interval of about 30–40 km is required to achieve notable improvements. This constraint makes the algorithm sensitive to the spatial variations of the VPRs. At least the criterion E becomes lower than 10% for a distance of about 85–90 km. This value appears to be the maximum distance beyond which the VPR identification algorithm no longer operates whatever the considered distance interval. In order to complement this finding, this maximum distance of identification has been estimated for different radar operating conditions and brightband characteristics: beamwidths $\theta_0 = 1°$ and 1.5°; elevation angle increments between successive PPI, $\Delta A = \theta_0$ and $\theta_0/2$; and brightband peaks at 1.5, 2.0, and 2.5 km above the radar. It should be noted that they remain purely indicative and valid in the theoretical context of the sensitivity tests. The results obtained have been listed in Table 2. They indicate that the maximum identification range varies from 70 km to 120 km or more depending on the conditions of the VPR identification. However, it appears that the maximum distance of the VPR identification depends mainly on brightband characteristics and less on radar operating conditions.

b. A priori VPR and associated covariance matrix

This influence has been assessed by comparing the initialization based on the apparent VPR to initializations based on a priori VPRs of different shapes (Andrieu et al. 1995). It clearly appears that choosing the discretized apparent VPR provided by radar data as the a priori VPR is the best. This conclusion can be explained by at least two reasons: i) the observed apparent VPR always remains not too far from the solution, and ii) the statistical distribution of residuals of the VPR components is unimodal or Gaussian, hence consistent with the assumptions of the inverse method. Concerning the covariance matrix, a standard deviation constant $\sigma_z = 0.7$ and a distance decorrelation $D_z = 0.6$ appear as the good compromise (Vignal 1998). An initial evaluation of this identification method is addressed in the next section, which presents a case study using actual radar data.

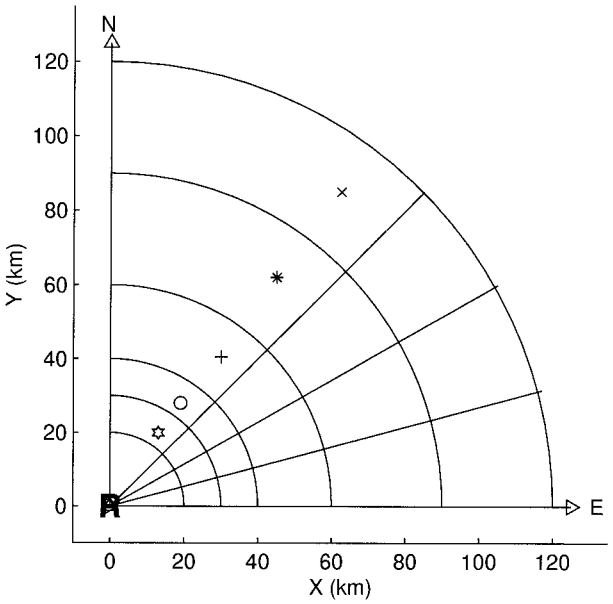

FIG. 8. Geographic sectors selected for testing the VPR identification method.

5. Case study

a. Presentation of data

Volume scan data from the C-band Monte Grande weather radar station, located in Italy, in the Venice region (Crespi and Monai 1991), have been used for this initial evaluation. A volume is composed of a series of 10 PPI at the following elevation angles: 0.5°, 1.0°, 1.5°, 2.5°, 3.5°, 3.5°, 4.5°, 6.0°, 7.5°, 10.0°, and 15.0°. The 3-dB radar beamwidth is 1° and the radar range is 120 km. The northeastern part of the radar umbrella, which is not polluted by ground detection, serves for the case study (Fig. 8). The considered dataset contains 12 h of data collected during a rain event that occurred on 4 October 1991 and displays large rainy zones as well as more convective rain cells. The studied rain event is illustrated by Fig. 9, which displays two PPI

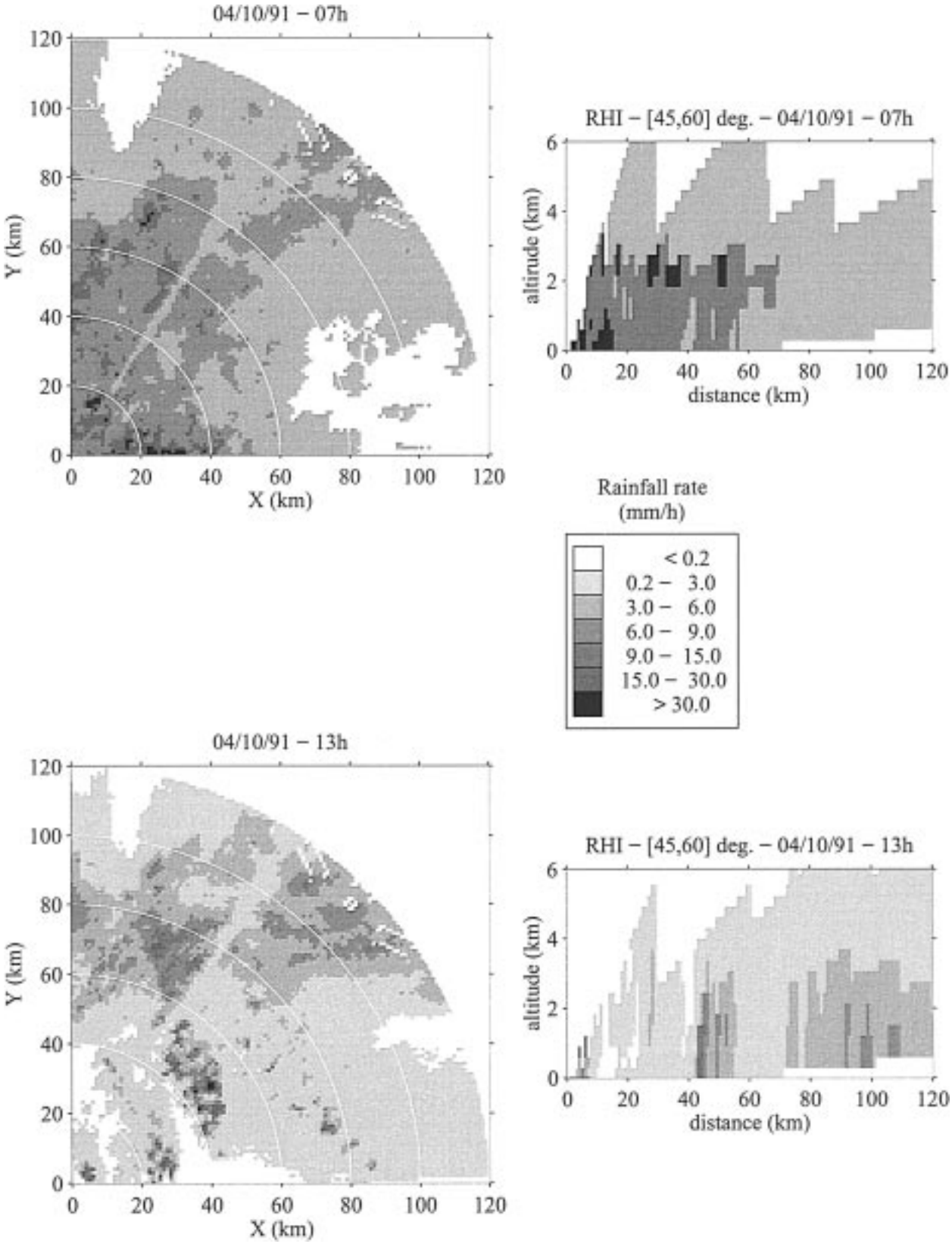

FIG. 9. Radar images recorded during the considered rain event. This images display hourly rainfall rates at different times, 7 h and 13 h. The left images represent CAPPIs at an altitude of 1 km, whereas the right images represent the mean RHIs in the azimuth sector (45°, 60°).

images and two RHIs taken from these PPIs, confirming the presence of rain periods with different characteristics. The average rainfall accumulation in the area of the radar umbrella studied here reaches 57 mm during this event. Measurements of radar reflectivities have been converted into rainfall intensities using the Marshall–Palmer relationship, $Z = 200R^{1.6}$. The evaluation of the VPR identification method uses radar data in the azimuth interval (45°, 90°).

b. Evaluation methodology

The direct means of testing the VPR identification would have been to compare identified VPRs to VPRs observed by a vertically pointing radar (Fabry and Zawadzki 1995). Since such a vertically pointing radar was not available in the present case study, an indirect means of evaluating the effectiveness of the VPR identification consists of checking whether this identification allows improvement in the radar rainfall measurement. This indirect evaluation nonetheless remains quite consistent with the main topic of interest in this work, an orientation toward the hydrological applications of radar data. In this light, the validation focuses on the rainfall accumulation at an hourly time step on surfaces of a few hundred square kilometers. This choice corresponds to the requirement of the hydrological modeling of catchments on this range of surface (Obled 1991).

The study domain is divided into 15 sectors (see Fig. 8) that serve to determine the VPRs. The sectors are 15° wide in azimuth. As suggested by the sensitivity tests (paragraph 4b), the distance interval increases with the mean distance from the radar. The VPR identification is performed at the sector scale and local VPRs do not have the same spatial representativity. Ratios of hourly rainfall measurements serve for the VPR identification. The parameter values of the identification procedure are listed in Table 1. An example of an identified VPR is provided in Fig. 10 that shows the a priori and identified VPRs, respectively (Fig. 10a), along with the ratio curves of observed radar data or corresponding to the identified VPR (Fig. 10b). The identified VPR displays a strong bright band at an altitude of 2 km, the echo-top level being at a height of 4.5 km. Figure 10a confirms that the identification makes it possible to obtain details on the strong vertical variations of the VPR, such as bright band, which are not visible in the apparent VPR captured by the radar. Figure 10b shows that the ratio curves associated with the identified VPR are very close to ratio curves observed, a result that confirms the accuracy of the determined VPR.

The VPR identification method has been tested according to the following approach.

1) Radar data recorded at the lowest elevation angle are considered as reference values. They are not used in the VPR identification procedure and serve only for validation purposes. Ratio curves are calculated from radar data at higher elevation angles.
2) Ratio curves of each geographic sector (see Fig. 8) are calculated in order to identify the relevant local VPR. The identification algorithm is initialized with the mean apparent VPR deduced from volume scan radar data from the considered geographic sector.
3) Once identified, the local VPR is then used to correct the raw radar data of the geographic sector. Radar data recorded at elevation angles of 1.0° and 1.5° serve to test the identification method. They are corrected for the influence caused by the VPR in order to agree with the reference radar data (elevation angle of 0.5°). To evaluate the improvement provided by the local VPR correction, a comparison with reference radar data is performed in four different cases:

   Case A: no correction for the VPR influence is applied;
   Case B: the correction is based on the identified local VPR;
   Case C: the correction is based on the observed ap-

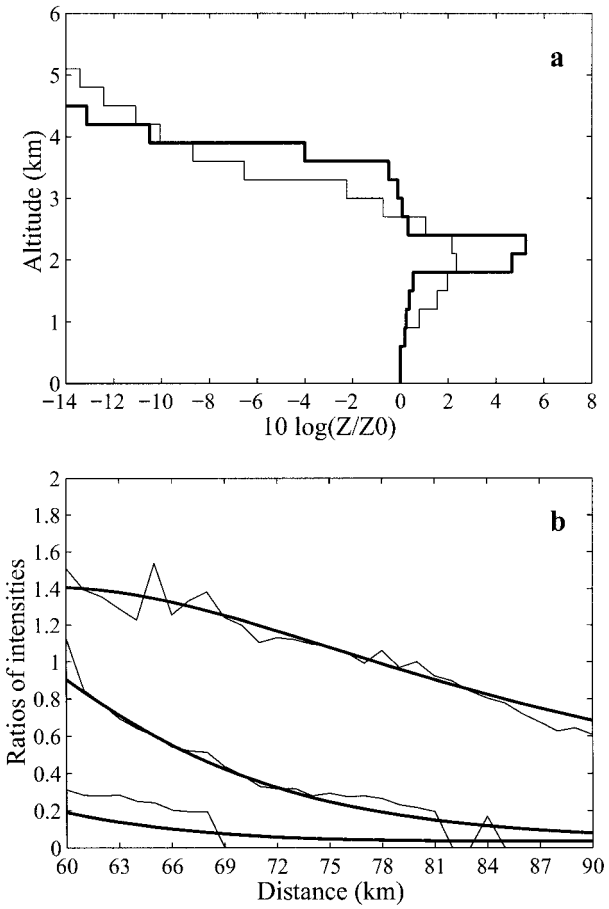

FIG. 10. Example of VPR identification from actual data between 60 and 90 km: 4 Oct 1991 at 0800 UTC. (a) A priori VPR (thin line) and identified VPR (thick line); (b) observed ratios of intensities (thin line) and ratios associated with the identified VPR (thick line).

parent VPR, which is used to initialize the identification method; and

Case D: the correction uses the mean VPR of the entire study zone, identified with mean ratio curves over the whole domain.

These different cases provide complementary insights into the efficiency of the VPR correction. A comparison of cases C and B allows evaluating the benefit of a radar correction based on identified VPRs compared to a correction based on apparent VPRs. A comparison of cases D and B serves to appreciate the value of taking account of the spatial variations of the VPR in the correction procedure. A comparison of cases B and A yields the overall efficiency of the tested VPR identification method.

The corrected values of radar data are obtained using the following expression:

$$Z^*(x, A_{\text{ref}}) = \overline{Z}(x, A)\frac{z_{Da}(x, A, \theta_0)}{z_{Da}(x, A_{\text{ref}}, \theta_0)}, \qquad (13)$$

where x is the distance, A is the elevation angle, and A_{ref} stands for the elevation angle of the reference radar measurement. Here, $\overline{Z}$ is the measured reflectivity, $z_{Da}(x, A, \theta_0)$ is the value of the apparent VPR in measurement conditions, and $z_{Da}(x, A_{\text{ref}}, \theta_0)$ represents the value of the apparent VPR in reference conditions, Z^* being the corrected radar measurement. Equation (13) is obtained by eliminating the reflectivity at ground level in Eq. (3) written for the measurement elevation angle A, and the reference elevation angle A_{ref}, respectively.

For the sake of simplicity, the root-mean-square deviation is the single criterion used in this validation procedure,

$$\text{rmsd} = \frac{\sqrt{\sum_{i=1}^{i=n_s}\sum_{j=1}^{i=n_t}(R_{ij}^{\text{tes}} - R_{ij}^{\text{ref}})^2}}{\sum_{i=1}^{i=n_s}\sum_{j=1}^{i=n_t}R_{ij}^{\text{ref}}}, \qquad (14)$$

where n_s and n_t are the number of geographic sectors and time steps, respectively. Here R^{ref} is the reference areal radar rainfall estimated at the elevation angle $A_{\text{ref}} = 0.5°$, and R^{tes} is the tested, uncorrected, areal radar rainfall estimation at elevation angles 1.0° and 1.5°.

c. Results of the validation

The inverse algorithm used in this study requires that the residuals between a priori and true values of data and parameters respect Gaussian statistical distributions. A very rigorous verification of this hypothesis is not possible, since the true values remain unknown. However, this hypothesis can be checked by assuming that identified VPRs and corresponding ratio curves are representative of truth values. Based on this assumption, Fig. 11 illustrates the statistical distributions of ratio residuals and VPR component residuals for the studied rain event. It confirms the mean value of these distributions is very close to 0.0, their standard deviation being 0.3 and 0.28. Moreover, Fig. 11 shows that these distributions are unimodal and symmetrical, and not very different from a normal law, thereby justifying the use of this algorithm (Menke 1989).

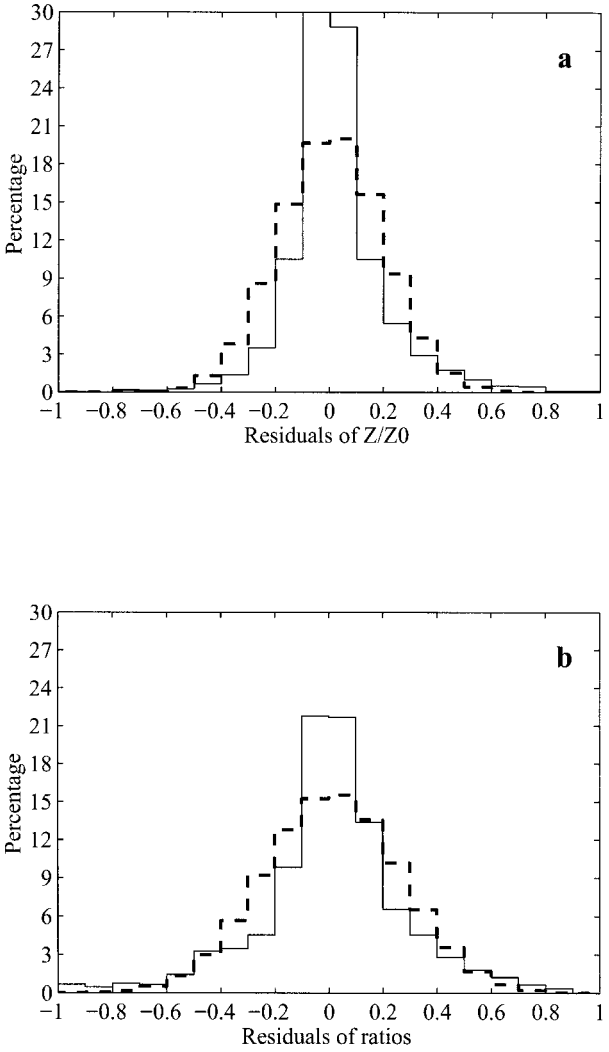

FIG. 11. Statistical distribution of the residuals (a) between a priori VPRs and identified VPRs; (b) between observed ratios of intensities and ratios corresponding to the identified VPRs. Continuous lines stand for observed distributions and dashed lines represent Gaussian distributions having the same mean and standard deviation.

The results of the hydrological validation have been combined in Table 3. The comparison of cases A and B shows that the correction of radar data for the influence of local VPR allows, in general, improvement of the measurement of rainfall. For radar data at an elevation angle of 1°, the improvement remains slight (rmsd of 11.5% vs 13.2%); these results can be explained by the small difference in elevation angle between the reference and tested values, which makes the

TABLE 3. Evaluation of the VPR identification method using 12 h of data recorded by the Monte Grande weather radar on 4 Oct 1991 (see section 5a). The criterion is the rmsd [defined in Eq. (14)] between reference and tested values of the radar rainfall measurement.

Sectors	All	20–30 km	30–40 km	40–60 km	60–90 km	90–120 km
Elevation angle: 1°						
No correction (A)	13.2%	10.2%	8.5%	8.8%	22.6%	10.0%
Identified (B)	11.5%	6.4%	6.0%	8.4%	7.2%	17.8%
Apparent (C)	12.2%	6.7%	7.2%	8.9%	9.1%	18.2%
Mean (D)	13.1%	7.2%	7.0%	9.7%	10.5%	19.3%
Elevation angle: 1.5°						
No correction (A)	43.2%	16.4%	13.5%	19.1%	31.4%	70.6%
Identified (B)	11.2%	8.9%	6.8%	11.2%	8.3%	15.2%
Apparent (C)	21.6%	8.9%	9.1%	14.0%	20.3%	32.6%
Mean (D)	25.3%	14.5%	12.9%	20.8%	22.5%	36.6%

VPR influence harder to detect. The more significant improvement, obtained for geographic sectors of the distance interval (60–90 km) (rmsd of 7.2% vs 22.6%) is unfortunately counterbalanced by the degradation observed in the farthest geographic sectors (rmsd of 17.8% instead of 10.0%); this degradation remains unexplainable. Concerning radar data at an elevation angle of 1.5°, the identification of local VPRs allows a very significant improvement in rainfall measurement (rmsd of 11.2% for corrected data compared to 43.2% for uncorrected data). Moreover, the correction efficiency increases with the distance to the radar and reaches a maximum for the farthest geographic sectors. These results are illustrated in Fig. 12, which shows the scattergram of radar data at 1.5° versus the reference radar data (0.5°) before correction (Fig. 12a) and after correction (Fig. 12c), respectively, for the local VPR influence. Figure 12a clearly illustrates the underestimation of the rainfall rate that occurs for the furthest radar data (90 km, 120 km) when they are not corrected (crosses). Though less obvious, the overestimation due to the presence of bright band in the radar beamwidth that mainly concerns measurements in the sectors between 60 and 90 km is also visible (stars in Fig. 12a). The correction of radar data from the VPR influence makes it possible to correct these two biases (Fig. 12c).

The second aspect of validation deals with the comparison of alternative possibilities: i) correction for the VPR influence using the discretized apparent VPR deduced from radar data (case C) or ii) correction for the VPR influence based on a mean VPR on the study zone (case D). These comparative results are presented in Table 3. They confirm that, in any event, a correction of radar data based on identified local VPRs is more accurate than corrections based on both of the methods considered herein. For radar data at an elevation angle of 1°, the gain remains again slight, due to the weak differences between corrected and uncorrected radar data. Note that all correction methods result in a degradation of radar measurements for the farthest geographic sectors (90–120 km). As previously mentioned, the gain allowed by considering identified local VPRs is more sensitive for radar data at a 1.5° elevation angle. In this case, results associated with identified VPRs and apparent discretized VPRs provided by volume scan radar data are similar for geographical sectors close to the radar (distance less than 40 km), for which the 1.5° radar beam does not sample the bright band. The advantage of identifying local VPRs becomes significant for distances larger than 40 km when bright band is included in the radar beam, as confirmed by the corresponding values of rmsd, 8.3% versus 20.3% for the geographic sectors 60–90 km, and 15.2% compared with 32.6% for the geographic sector 90–120 km. The comparison between scattergrams shown in Figs. 12b and 12c illustrates this conclusion. In the same manner, corrections based on identified local VPRs appear to be more accurate than those using the mean global VPR.

6. Conclusions

This article has extended to volume scan radar data a VPR identification method that was previously designed for the particular case of radar data at two elevation angles. This extension allows, in particular, the identification of local VPRs. The application conditions of the identification method have been defined in order to provide complementarity to the discretized VPR directly determined from volume scan radar. Indeed, the VPR identification enables refining this discretized VPR. Sensitivity tests have been performed to correctly parameterize the extended method. The validation of this method has been carried out through a case study by adopting an approach suited to hydrological applications. This hydrological validation consists of checking if the correction of radar data for the VPR influence improves the measurement of rainfall by radar. The results obtained can be summarized as follows. In the context of the case study, taking account of the VPR influence through the identification of local VPRs improves the accuracy of radar data. Moreover, a correction of radar data based on the identification of local VPRs appears more efficient than both: i) a correction for a mean VPR and ii) a correction based on discretized apparent VPRs deduced from volume scan radar data. These obtained results are quite encouraging although

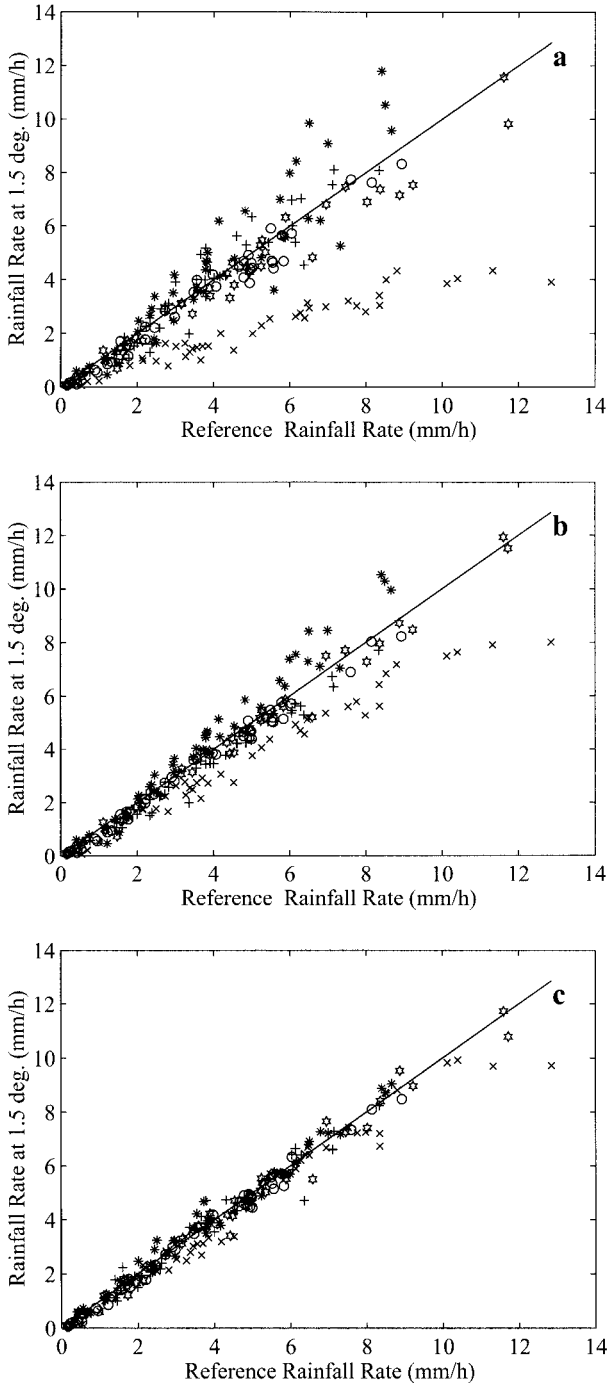

FIG. 12. Scattergram reference radar data vs radar data at an elevation angle of 1.5° in three different cases: (a) radar data are not corrected for the VPR influences; (b) the correction for the VPR influence uses the apparent VPR deduced from observed radar data; (c) the correction for the VPR influence is based on identified local VPRs. The markers are associated with geographic sectors (see Fig. 8).

a more rigorous validation using a larger set of radar data recorded under different meteorological conditions is necessary. More specifically, it would be interesting to apply the VPR identification method i) to rain events displaying a stronger spatial variability of VPRs, such as groups of convective rain cells in various stages of lifetime, and ii) to more complex mesoscale systems having both convective and stratiform precipitation components. Additionally, the study of the spatial variations of VPRs would make it possible to determine the surface areas over which a VPR can be considered invariant for different rain types and would contribute to better define the application conditions of the proposed method.

The method evaluation has been limited to the framework of hydrological applications requiring hourly rainfall measurements. Thus, identified VPRs are representative of vertical variations of reflectivity at a hourly time step. It would be valuable to continue investigations toward the identification of quasi-instantaneous VPR. From a scientific point of view, this would open the path to deducing the true VPR from volume scan radar data or from RHI, thereby making it possible to study the spatial variability of VPRs. As far as applications are concerned, the availability of quasi-instantaneous VPRs is of importance in urban hydrology where very short timesteps are required. Moreover, very short-term rainfall forecasting methods that use the vertically integrated rainwater content (VIL) are being developed (see French and Krajewski 1994, for instance). The availability of an accurate VPR could be a necessary condition to improving the VIL estimation, to better discriminate between ice and liquid water in the rain profile, for example. The extension of the VPR identification method to instantaneous VPRs encounters at least two difficulties: i) the problem of rainfall intermittence in the study zone that affects the calculation and the representativity of the ratio curves and ii) the need for a direct evaluation of the method consisting in comparing identified VPRs to VPRs observed by a vertically pointing radar. However, this direct evaluation would certainly introduce new difficulties, related to the spatial representativity of the very punctual VPRs provided by the vertically pointing radar.

Acknowledgments. This work was supported by the Commission of the European Communities, DG XII, Environment and Climate Program, Project HYDROMET, Contract ENV 4CT 960290. The authors thank Marco Monai (CSIM) and Marco Borga (University of Padova) for providing the radar data used in the paper and helpful discussions. They would like to thank Dr. Jurg Joss and two anonymous reviewers who provided very helpful comments and suggestions to improve the paper.

REFERENCES

Andrieu, H., and J. D. Creutin, 1991: Effect of the vertical profile of reflectivity on the rain assessment at the ground level. Preprints,

25th Int. Conf. on Radar Meteorology, Paris, France, Amer. Meteor. Soc., 832–835.

——, and ——, 1995: Identification of vertical profiles of radar reflectivity using an inverse method: 1—Formulation. *J. Appl. Meteor.*, **34,** 225–239.

——, G. Delrieu, and J. D. Creutin, 1995: Identification of vertical profiles of radar reflectivity using an inverse method: 2—Sensitivity analysis and case study. *J. Appl. Meteor.*, **34,** 240–259.

——, J. D. Creutin, G. Delrieu, and D. Faure, 1997: Use of a weather radar for the hydrology of a mountainous area. Part 1: Radar measurement interpretation. *J. Hydrol.*, **193,** 1–25.

Borga, M., E. N. Anagnostou, and W. F. Krajewski, 1997: A simulation approach for validation of a brightband correction method. *J. Appl. Meteor.*, **36,** 1507–1518.

Collier, C. G., 1986: Accuracy of rainfall estimates by radar, Part 1: Calibration by telemetering raingages. *J. Hydrol.*, **93,** 207–223.

Crespi, M., and M. Monai, 1991: Some remarks on precipitation measurements with a Doppler radar. Preprints, *25th Int. Conf. on Radar Meteorology*, Paris, France, Amer. Meteor. Soc., 323–325.

Fabry, F., and I. Zawadzki, 1995: Long-term radar observations of the melting layer of precipitation and their interpretation. *J. Atmos. Sci.*, **52,** 838–850.

——, G. L. Austin, and T. Tees, 1992: The accuracy of rainfall estimates by radar as a function of range. *Quart. J. Roy. Meteor. Soc.*, **118,** 435–453.

French, M. N., and W. F. Krajewski, 1994: A model for real-time quantitative rainfall forecasting using remote sensing. 1. Formulation. *Water Resour. Res.*, **30,** 1075–1083.

Hardaker, P. J., A. R. Holt, and C. G. Collier, 1995: A melting layer model and its use in correcting for the brightband in single polarization radar echoes. *Quart. J. Roy. Meteor. Soc.*, **121,** 495–525.

Joss, J., and A. Waldvogel, 1990: Precipitation measurement and hydrology. *Radar in Meteorology: Battan Memorial and 40th Anniversary Radar Meteorology Conference*, D. Atlas, Ed., Amer. Meteor. Soc., 577–606.

——, and R. Lee, 1995: The application of radar-gauge comparisons to operational precipitation profile corrections. *J. Appl. Meteor.*, **34,** 2612–2630.

Kitchen, M., R. Brown, and A. G. Davies, 1994: Real-time correction of weather radar data for the effects of brightband, range and orographic growth in widespread precipitation. *Quart. J. Roy. Meteor. Soc.*, **120,** 1231–1254.

Klaassen, W., 1988: Radar observations and simulation of the melting layer of precipitation. *J. Atmos. Sci.*, **45,** 3741–3753.

Koistinen, J., 1991: Operational correction of radar rainfall errors due to the vertical reflectivity profile. Preprints, *25th Int. Conf. on Radar Meteorology*, Paris, France, Amer. Meteor. Soc., 91–96.

Menke, W., 1989: *Geophysical Data Analysis*: *Discrete Inverse Theory.* Academic Press, 260 pp.

Obled, C., 1991: Reflections on rainfall informations required for operational rainfall-runoff models. *Hydrological Applications of Weather Radar*, I. D. Cluckie and C. G. Collier, Ed., Ellis Horwood, 469–482.

Tarantola, A., 1987: *Inverse Problem Theory.* Elsevier, 613 pp.

——, and B. Valette, 1982a: Generalized nonlinear inverse problem solved using the least squares criterion. *Rev. Geophys. Space Phys.*, **20,** 219–232.

——, and ——, 1982b: Inverse problems: Quest for information. *J. Geophys.*, **50,** 159–170.

Vignal, B., 1998: Mesure des précipitations par radar: Influence de la résolution du faisceau et de l'atténuation. Identification par méthode inverse des profils verticaux de réflectivité et des profils radiaux d'atténuation. Ph.D. thesis, Institut National Polytechnique de Grenoble, 233 pp.